The influence of curst-mantle constrain on the mineralization of orogenic gold deposits in the southeastern Ailaoshan metallogenic belt, SW China: Insights from 3-D magnetotelluric imaging

Zhe Yun[1], Zhiguo An[2], Qingyun Di[2], Pengfei Liang[2], Ya Gao[2], Yilang Zhang[1]
1.College of Earth and Planetary Sciences, University of Chinese Academy of Sciences, CAS Engineering Laboratory for Deep Resources Equipment and Technology, Institute of Geology and Geophysics, Chinese Academy of Sciences, Beijing 100029, China
yz791161833@163.com
zhangyilang20@mails.ucas.ac.cn
2.CAS Engineering Laboratory for Deep Resources Equipment and Technology, Institute of Geology and Geophysics, Chinese Academy of Sciences
zgancas@mail.iggcas.ac.cn
qydi@mail.iggcas.ac.cn
liangpngfei@outlook.com
gaoya@mail.iggcas.ac.cn

SUMMARY

The Ailaoshan-Red River mafic belt, as a suture zone of convergent accretionary processes in India and Asia since the early Cenozoic, was also an orogenic gold belt formed in a unique collisional context. To explore the mineralization in the southeastern Ailaoshan metallogenic belt on the southeastern margin of Tibet, the electrical resistivity structure model of the lithosphere was obtained through 3D inversion of magnetotelluric data. The preferred model indicated that the electrical structure of the upper crust was interlaced with high and low resistivity, and two stratified and massive conductors existed in the lower crust and upper mantle. Additionally, these conductors were continuously distributed in the transverse direction and extended deep in the vertical direction, we suggested that these conductors provided southeastern Ailaoshan metallogenic belt essential heat and molten ore-forming fluid. Moreover, four resistors encircled the shallow conductor at upper crustal depths may prompt the ore-forming fluid upwelling along the fault zones, which facilitates the enrichment of mineral fluids into the upper crust and upward intrusion into storage space in the form of veins.
Keywords: lithospheric electrical structure, magnetotelluric, 3-D inversion, orogenic gold deposit

INTRODUCTION

Tectonically, the Sanjiang Tethys metallogenic domain (STMD) was located in the eastern part of the Himalayan-Tibetan orogenic belt in the Sanjiang Tethys of south-west China, and although it was formed in the Early Palaeozoic, there was extensive metallogenesis in the Late Palaeozoic, Late Triassic and Himalayan (Tertiary). Important gold, copper, base metal, rare metal and tin ore belts have been developed in the area, and there are a large number of giant ore deposits [*Deng et al.*, 2014; *Hou et al.*, 2007]. Ailaoshan metallogenic belt was the most important Himalayan orogenic gold belt in China, which was formed in the process of Sanjiang Tethys composite orogeny. The Allaoshan was the largest orogenic gold belt in southwestern China, located on the southeastern margin of the Tibetan Plateau, which built on a tectonic collage of continental blocks, including the Sibumasu, Indochina and Yangtze blocks, which were merged as a result of the closure of the Triassic Paleo-Tethyan and the Cenozoic Neo-Tethyan [*Yin and Harrison*, 2000]. Its tectonic evolution was mainly controlled by the Cenozoic Indo-Asian collision, which resulted in a large number of strike-slip faults with block extrusion and Eocene-Miocene magmatism, such as Ailaoshan Red River Fault (AL-RRF), Xiaojiang Fault (XJF) and Dian Bien Phu Fault (DBFF) (Figure 1a). The ore fluids of Ailaoshan gold belt although contentious [*Goldfarb and Groves*, 2015], were argued to have been derived from a sub-crustal source, and have strong correlation with deep lithospheric material composition [*Wyman et al.*, 2016].

The observation results of geophysical data in this area revealed that there was a wide range of low velocity [*Bao et al.*, 2015], low resistivity [*Li et al.*, 2019; *Yu et al.*, 2020], strong seismic wave attenuation [*Chen et al.*, 2014], strong anisotropy [*Cai et al.*, 2016], high Poisson's ratio [*Hu et al.*, 2018] and Bouguer gravity anomaly disequilibrium [*Shen et al.*, 2022] in this area. These physical characteristics all indicated the complexity of the stratigraphic structure in the study area and the inhomogeneity of the material composition in the deep crust and mantle. Although not definitive, the isotopic signatures of sulfur and oxygen for the orogenic gold deposits imply mantle derivation of

the auriferous ore fluid. However, the nature of mantle–crust architecture and its tectonic drivers, especially the nature of the control by lithosphere on the orogenic gold deposits, was not previously well defined [*Hou et al.*, 2023]. In view of this, it was essential to study the upper mantle upwelling and associated crust-mantle interaction in the Ailaoshan metallogenic belt, the lithospheric electrical structure obtained by us can provide an improved understanding of orogenic gold deposits' metallogenic mechanism.

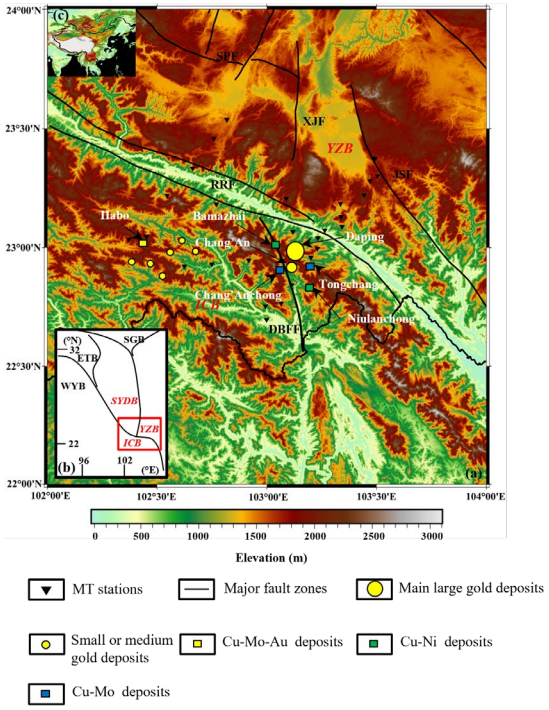

Figure 1 (a)Topographic map and distribution of MT stations in the study area. (b) Plate tectonic location in the study area [*Z Xu et al.*, 2011]. (c)Schematic distribution of the study area in China. The black line was the main fault zone in the study area, different coloured squares represented different ore concentration areas, and yellow circles represented gold deposits [*Hou et al.*, 2023; *Yang et al.*, 2023].

METHODS

3D Electrical Resistivity Model

Magnetotelluric (MT) was a frequency domain electromagnetic method for imaging the deep structure of the earth using naturally varying electromagnetic fields as the field source. In this study, we inverted broadband MT data in the study area (Figure 1a) to obtain a 3D resistivity model of the southeastern Ailaoshan metallogenic belt and its surrounding areas. 27 MT stations were laid, the frequency range was 0.003-3000s, the distance between the survey points was 5km-10km, and several discrete points were designed between the survey lines. The DRU electromagnetic receiving system developed by the Institute of Geology and Geophysics, Chinese Academy of Sciences [*Di et al.*, 2013] was used for this magnetotelluric data collection.

In this study, the 3D model was inverted based on ModEM [*Kelbert et al.*, 2014], we inverted the full impedance tensor from the 27 broadband MT stations. MT data used in the inversions were interpolated at 29 frequency points equally spaced in the logarithmical scale at 0.03–3000s. The error floors for diagonal elements were set to 10% of $|Zxy \cdot Zyx|^{1/2}$, while 5% of $| Zxy \cdot Zyx|^{1/2}$ was used for the off-diagonal elements. The central area of the study area was 130x100km and was discrete into horizontal cells of 1x1 km, and the extended area was filled with 9 grids with a scale factor of 1.5. In the vertical direction, the thickness of the first layer was 20 m with a scale factor of 1.2, and the maximum thickness was 56km. The entire modelling volume is 350km×330km×188km, and the grid had 118×142×39 cells in the x, y and z directions, respectively. A starting model of 100 Ωm was used with a model covariance factor of 0.3 in all directions. Finally, we obtained the preferred model with an RMS (root-mean-square) misfit from 11.1438 to 2.1313 after 400 iterations (Figure 2).

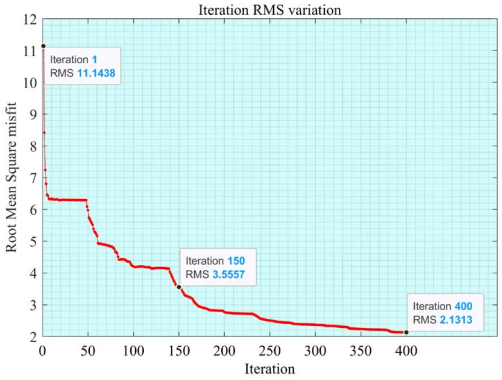

Figure 2 RMS misfit in the preferred model from 3-D inversion

RESULTS

As shown in Figure 3, the electrical structure in the upper crust (Figure 3a-b) was characterized by transverse inhomogeneity. Some high conductors (C1, C2) were divided by resistive bodies (R1, R2, R3 and R4), and the exposure range of C3 and C4 increased with depth. C4 may represented the distribution of the Haber Cu-Mo-Au deposits in the upper crust. In the middle crust (Figure 3c-d), the lateral extension of high conductors becomes larger, and the high conductors C1 and C2 are connected , in which C1 and C2 may be the source of deep mineral fluids for the daping gold deposits and its surrounding polymetallic deposits. In the lower crust (Figure 3e-f), only high conductors C1 and C3 were formed into bands in a wide range, and they tended to be interconnected, which may be due to the effect of deep hot materials in the lower crust, and the

transverse inhomogeneity of the electrical structure was weakened.

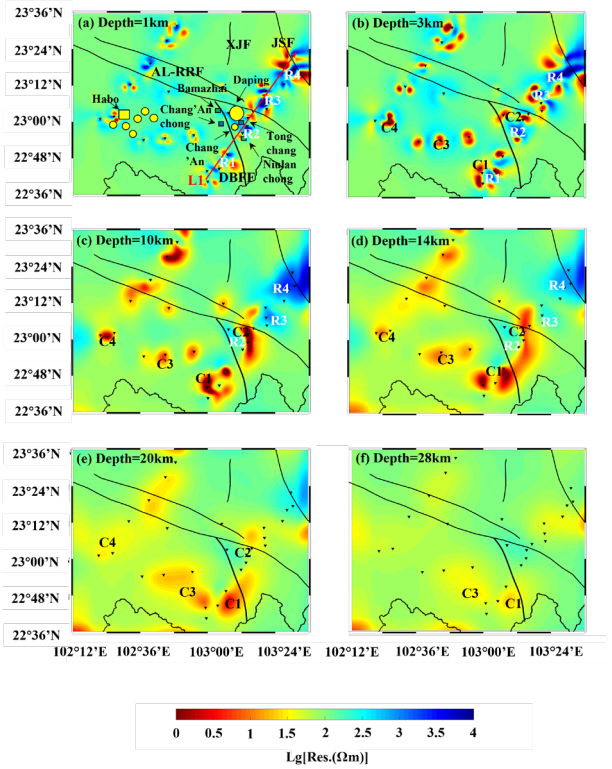

Figure 3. Horizontal slices of the 3-D MT model in the southeastern Ailaoshan metallogenic belt at different depths.The resistive bodies were denoted by R, and the high conductor bodies were denoted by C. The black line was the main fault zone in the study area, and the red line was the L1 profile in the study area, other identifiers are consistent with Figure 1.

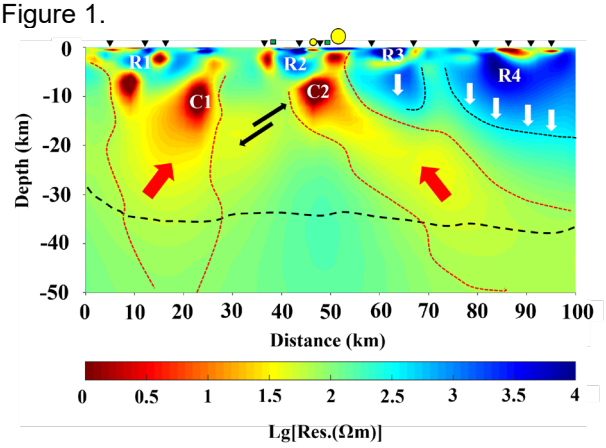

Figure 4. Vertical electrical structure of L1 profile. The red arrow represented the projected movement of heated material in the lower crust, and the white arrow represented the barrier effect of the resistive bodies, whereas the black arrow showed the flow direction for substances with high conductors. The red dotted line represented a deep mineral upwelling channel, and the black dotted line represented impermeable boundaries. The black triangle represented the MT stations.

As shown in Figure 4, L1 was the vertical section of the resistivity model from northwest to southeast. C1 and C2 were distributed in bands and extended downward throughout the crust, forming two hydrothermal ascending channels (red arrow in Figure 4), and there may be a hot material exchange between 15km and 25km (black arrow in Figure 4). The source of heat flow was likely to be the lateral migration of hot material in the crust flow and the upwelling of deep molten material in the Hainan mantle plume along the nearby fault zone [*Yu et al.*, 2020]. Moreover, the R3 and R4 were presumably the consequence of hot material eroding the high speed [*Zhang et al.*, 2020], high resistivity and density crust [*Shen et al.*, 2022] in the Emeishan Large Igneous Province[*Y G Xu et al.*, 2004]. R3 and R4 provided impermeable boundaries for mineral fluid enrichment, making deep molten mineral fluid upwelling along the nearby fault zone.

CONCLUSIONS

The study area of this paper was located in the southeastern Ailaoshan metallogenic belt and its neighbouring areas on the southeast margin of the Tibetan Plateau. The three-dimensional electrical structure of the southeastern Ailaoshan metallogenic belt was provided, and the deep crust-mantle electrical structure of the region was analysed, as well as the influence of crust-mantle interaction on the mineralization mechanism. The electrical structure of the southeastern Ailaoshan metallogenic belt showed a high and low resistivity staggered distribution, with a large range of layered and massive high-conductivity anomalies in the upper crust and the lower crust, some of which were distributed continuously in the transverse direction and had a tendency to extend to the depth in the vertical direction. We speculated that there may be two ore-fluid channels formed by deep molten materials, and there may be mineral element exchange in the middle and lower crust of different mining areas.

ACKNOWLEDGEMENTS

The authors thank the reviewers and editors for their detailed comments on this article. This research is supported by the Strategic Priority Research Program of the Chinese Academy of Sciences (Grant No. XDA0430103 and No.XDA0430301) and the National Key Research and Development Program of China (Grant No.2023YFB3905005), and the data source is provided by Professor Di. We thank GMT and MTpy for the package and we thank Prof. Gary Egbert for the use of ModEM software.

REFERENCES

Bao, X., X. Sun, M. Xu, D. W. Eaton, X. Song, L. Wang, Z. Ding, N. Mi, H. Li, and D. Yu (2015), Two crustal low-velocity channels beneath SE Tibet revealed by joint inversion of Rayleigh wave dispersion and receiver functions, *Earth and Planetary Science Letters*, *415*, 16-24.

Cai, Y., J. Wu, L. Fang, W. Wang, and S. Yi (2016), Crustal anisotropy and deformation of the southeastern margin of the Tibetan Plateau revealed by Pms splitting, *Journal of Asian Earth Sciences*, *121*, 120-126.

Chen, M., H. Huang, H. Yao, R. van der Hilst, and F. Niu (2014), Low wave speed zones in the crust beneath SE Tibet revealed by ambient noise adjoint tomography, Geophysical Research Letters, 41(2), 334-340.

Chen, Y., Z. Zhang, C. Sun, and J. Badal (2013), Crustal anisotropy from Moho converted Ps wave splitting analysis and geodynamic implications beneath the eastern margin of Tibet and surrounding regions, Gondwana Research, 24(3-4), 946-957.

Deng, J., Q. Wang, G. Li, C. Li, and C. Wang (2014a), Tethys tectonic evolution and its bearing on the distribution of important mineral deposits in the Sanjiang region, SW China, Gondwana Research, 26(2), 419-437, doi:https://doi.org/10.1016/j.gr.2013.08.002.

Di, Q.-Y., G.-Y. Fang, and Y.-M. Zhang (2013), Research of the Surface Electromagnetic Prospecting (SEP) system, Chinese Journal of Geophysics-Chinese Edition, 56(11), 3629-3639, doi:10.6038/cjg20131104.

Goldfarb, R. J., and D. I. Groves (2015), Orogenic gold: Common or evolving fluid and metal sources through time, Lithos, 233, 2-26, doi:https://doi.org/10.1016/j.lithos.2015.07.011.

Hou, Z., Q. Wang, H. Zhang, B. Xu, N. Yu, R. Wang, D. I. Groves, Y. Zheng, S. Han, and L. Gao (2023), Lithosphere architecture characterized by crust–mantle decoupling controls the formation of orogenic gold deposits, *National Science Review*, *10*(3), nwac257.

Hou, Z., K. Zaw, G. Pan, X. Mo, Q. Xu, Y. Hu, and X. Li (2007), Sanjiang Tethyan metallogenesis in S.W. China: Tectonic setting, metallogenic epochs and deposit types, *Ore Geology Reviews*, *31*(1), 48-87, doi:https://doi.org/10.1016/j.oregeorev.2004.12.007.

Hu, J., J. Badal, H. Yang, G. Li, and H. Peng (2018), Comprehensive crustal structure and seismological evidence for lower crustal flow in the southeastern margin of Tibet revealed by receiver functions, *Gondwana Research*, *55*, 42-59, doi:https://doi.org/10.1016/j.gr.2017.11.007.

Kelbert, A., N. Meqbel, G. D. Egbert, and K. Tandon (2014), ModEM: A modular system for inversion of electromagnetic geophysical data, *Computers & Geosciences*, *66*, 40-53.

Li, X., D. Bai, X. Ma, Y. Chen, I. M. Varentsov, G. Xue, S. Xue, and I. Lozovsky (2019), Electrical resistivity structure of the Xiaojiang fault system (SW China) and its tectonic implications, *Journal of Asian earth sciences*, *176*(JUN.1), 57-67.

Shen, Y. T., G. L. Yang, H. B. Tan, J. P. Wang, M. H. Zhang, and C. Y. Shen (2022), Review on Bougue gravity anomaly and crustal density structure in Sichuan-Yunnan and its adjacent areas, *Reviews of Geophysics and Planetary Physics*, *53*(3), 316-330, doi: 10.19975/j.dqyxx.2022-001.

Wyman, D. A., K. F. Cassidy, and P. Hollings (2016), Orogenic gold and the mineral systems approach: Resolving fact, fiction and fantasy, *Ore Geology Reviews*, *78*, 322-335, doi:https://doi.org/10.1016/j.oregeorev.2016.04.006.

Xu, Z., J. Yang, H. Li, S. Ji, Z. Zhang, and Y. Liu (2011), On the Tectonics of the India-Asia Collision, *Acta Geologica Sinica*, *85*(1), 1-33.

Xu, Y. G., B. He, S. L. Chung, M. A. Menzies, and F. A. Frey (2004), Geologic, geochemical, and geophysical consequences of plume involvement in the Emeishan flood-basalt province, *Geology*, *32*(10), 917-920

Yang, X.-A., J. Wu, D.-R. Xu, and H.-B. Ren (2023), Application of integrated geological and structural investigations to the discovery of new mineral zones related to the Daping gold deposit, Southwest China, *Ore Geology Reviews*, *158*, 105519, doi:https://doi.org/10.1016/j.oregeorev.2023.105519.

Yin, A., and T. M. Harrison (2000), Geologic evolution of the Himalayan-Tibetan orogen, *Annual Review of Earth and Planetary Sciences*, *28*, 211-280, doi:10.1146/annurev.earth.28.1.211.

Yu, N., M. Unsworth, X. Wang, D. Li, E. Wang, R. Li, Y. Hu, and X. Cai (2020), New insights into crustal and mantle flow beneath the Red River Fault zone and adjacent areas on the southern margin of the Tibetan Plateau revealed by a 3‐D magnetotelluric study, *Journal of Geophysical Research: Solid Earth*, *125*(10), e2020JB019396.

Zhang, Z. Q., H. J. Yao, and Y. Yang (2020), Shear wave velocity structure of the crust and upper mantle in Southeastern Tibet and its geodynamic implications, *Science China-Earth Sciences*, *63*(9), 1278-1293, doi:10.1007/s11430-020-9625-3.